Case Studies in Structural Engineering 4 (2015) 26–38

Contents lists available at ScienceDirect

Case Studies in Structural Engineering

journal homepage: www.elsevier.com/locate/csse

Case Study

Hand verification for flexural strength of existing R.C. floors subject to degradation phenomena

G. Campione*, F. Cannella, L. Cavaleri

DICAM, University of Palermo, Viale delle Scienze, 90128 Palermo, Italy

ARTICLE INFO

Article history:
Received 28 May 2015
Received in revised form 14 June 2015
Accepted 18 June 2015
Available online 24 June 2015

Keywords:
T beam
R.C. floor
Arch strength mechanism
Corrosion
Bond
Pitting

ABSTRACT

In the present paper, a simplified model for hand verification of the flexural and shear strength of existing corroded T beams cast in place of lightened R.C. orthotropic slabs forming floors is presented and discussed. Diffused and pitting corrosion on steel bars, compressive concrete strength degradation and concrete bond strength degradation are included in the model. The original contribution of the paper is evaluation of the flexural and shear strength considering both the cases of strain compatibility and absence of compatibility and considering the main parameters governing the corrosion process. An arch-resistant model for the calculus of the flexural and shear strength of the beam was adopted in the absence of strain compatibility, while the plane section theory was adopted for the case of strain compatibility. No punching shear is considered. This approach is simple and can be applied on the basis of the experimental information available (carbonation test, chloride content, measurement of the pitting in the bar, gravimetric method for general corrosion) or by utilizing analytical expressions calibrated on the knowledge of the corrosion current intensity determined by linear polarization resistance measurement (LPR). The model was also verified against experimental results recently obtained by the authors.

1. Introduction

One of the most common types of orthotropic slab utilized in the Mediterranean area to form floors, between 1930 and 1970, was the type constituted by low thickness reinforced concrete beams having a T cross-section placed at a distance of between 200 and 500 mm and lightened with interposition of brick blocks (see Fig. 1). Fig. 1 shows a section of the slab construction, as indicated in textbooks of the past 50 years (e.g. [1]), with the typical arrangement of the steel reinforcements. The slab was constituted with reinforced concrete beams cast in place and having a T cross-section placed at intervals of 310 mm. The height of each beam was 170 mm (a value which respects the limit of minimum thickness of 1/30 of the span adopted in [1]). Each T beam was formed by a web of 70 mm and a height of 120 mm and an upper flange with minimum thickness 40 mm. Among the T elements brick blocks were placed, 120 mm high, 240 mm wide and 250 mm deep. The T beams were reinforced with smooth bars in the tension zone with straight or hook anchourages. The minimum percentage of steel reinforcement to be placed in the tensile zone was 0.25% of the cross-section area of concrete. The steel reinforcement was constituted by two bars of small diameter for each T beam. In the first two decades of the century it was common to adopt one straight bar and one bent one (see Fig. 1). In the second two decades of the century, it became common to

* Corresponding author. Tel.: +39 3204395955; fax: +39 091427121.
E-mail address: giuseppe.campione@unipa.it (G. Campione).

http://dx.doi.org/10.1016/j.csse.2015.06.001

List of symbols

A_s	cross-section area of longitudinal bars
b_f	beam width increased by corrosion cracking
b	beam section width in the virgin state
δ	concrete cover thickness
ϕ	bar diameter
ϕ_{red}	reduced bar diameter
f_c	mean value of concrete compressive strength
f_y	yield stress of longitudinal bar (or tie)
K	coefficient related to concrete
n_{bars}	number of bars in one layer
n	number of bars in the support
$u_{i\ corr}$	opening of corrosion crack
w_{cr}	total crack width for one corrosion level
X	corrosion attack depth
A_{pit}	bar cross-section area reduction due to pitting
ε_0	strain at peak compressive stress
q_{res}	residual bond strength
B	distance from each T beam
H	height of each beam
L	maximum span
l_{anc}	anchorage length
s	minimum thickness of the upper flange
a	shear span
j	dimensionless internal arm
P_{max}	maximum value of pit penetration
P_{av}	medium value of pit penetration

adopt two straight bars. The concrete cover thickness was 20 mm. The shaped bar was bent at 1/5 of the span, a length corresponding to the zero point of bending moment of a fixed beam subjected to a uniform distributed load.

In the flange of the T beam secondary steel reinforcements having a small diameter (4 or 6 mm) were placed, equivalent to 20% of the main reinforcement. No specific shear steel reinforcements were adopted in this type of structure. The shear force at the supports was provided by the web which, if necessary, was increased in thickness. This increase was made possible by not placing brick blocks in this zone.

In the first four decades of the century the maximum span adopted for this type of structure was between 3000 and 4000 mm, while more recently with a thickness of the T beam of 200 mm the span was between 5000 and 6000 mm.

Corrosion phenomena are caused by the loss of the protection provided by the concrete when carbonation occurs. Another cause of corrosion is the presence of chlorides. Carbonation and corrosion phenomena produce concrete cover spalling and reduction in the steel area. In some cases the damage is not too severe (see Fig. 2a and b) to be visible and needs external inspection; if more severe damage occurs, it is evident, from Fig. 2c and d and it is also dangerous for the safety of people. In all these cases safety assessment under current conditions is crucial. In some cases it is necessary to design retrofitting of structures to reproduce the initial safety conditions.

For safety assessment the deterioration and decay of materials must be taken into account [2–5]. This information can be obtained through destructive testing on materials (visual inspection, depth of carbonation, chloride content, gravimetric tests on the bars, measuring the depth of the pit, the corrosion current density on the bar measured experimentally, e.g. using linear polarization resistance measurement LPR [6], and non-destructive testing on structures (loading tests)).

For the analytical prevision of safety conditions the first problem that arises is the choice of a suitable calculation model, which in many cases of severe damage may not be the sectional model because of the loss of bond. The second problem is the choice of the confidence factor (CF), which depends on the level of detail and extent of the investigations.

Another important question not analyzed in the present paper, but of sure interest in future researches, could be the choice of the safety factor (or strength reducing factors) and their calibration. To do this the statistical aspect of parameters influencing the corrosion processes should be know.

The current research referred to the real cases analyzed by the writers in relation to R.C. buildings existing for the past 50 years in the Italian territory and in the province of Palermo. For these structures, it was observed that in the presence of aggressive environments about 25% of the ceilings of the basement and 35% of the ceilings of the roof of the building are affected by corrosion and carbonation processes. These phenomena are also influenced by the low cover thickness adopted, which was between 7 and 24 mm.

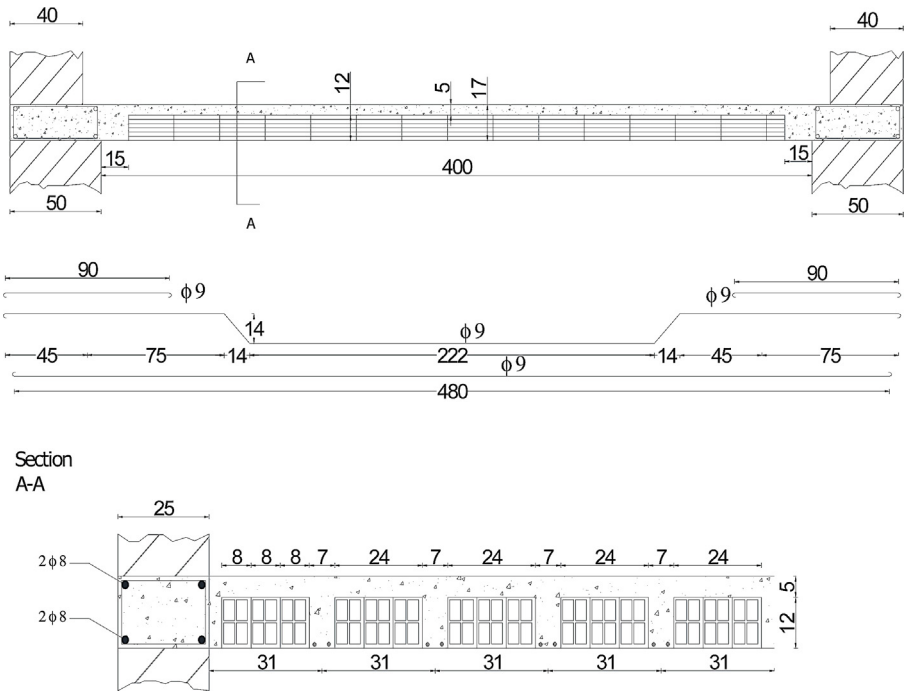

Fig. 1. Constructive section of R.C. floor according to Santarella [1].

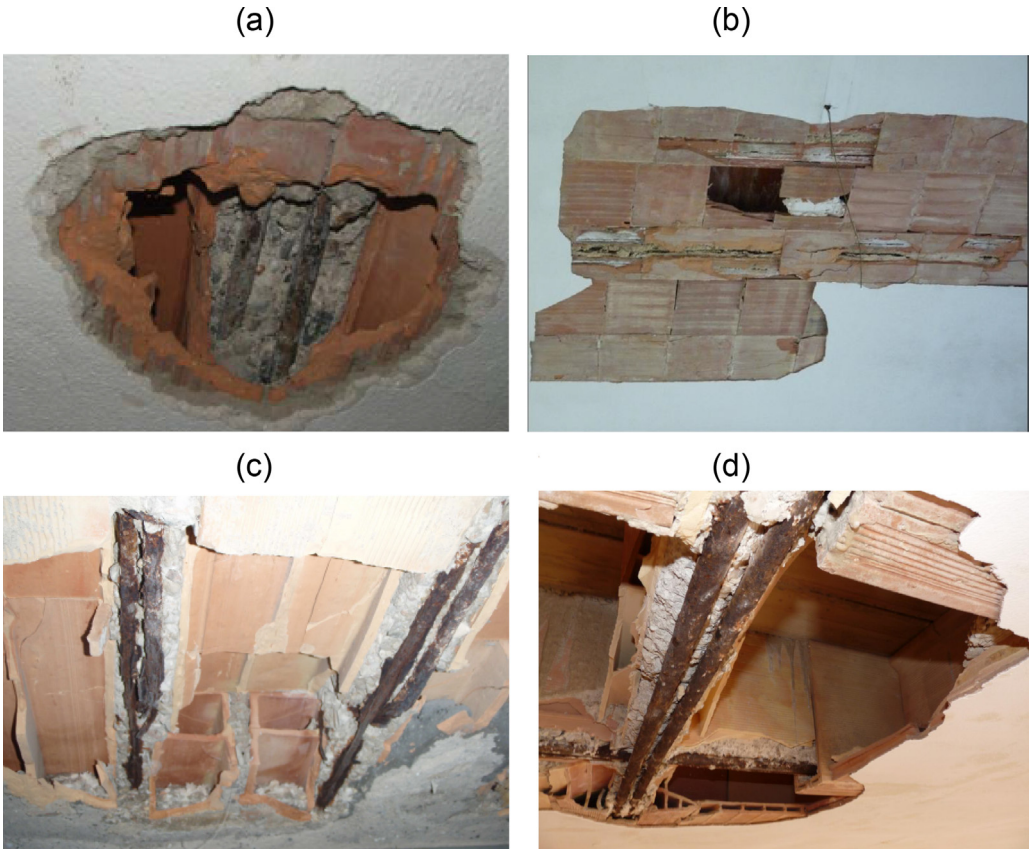

Fig. 2. Degradation phenomena in R.C. floors due to carbonation and chloride attack.

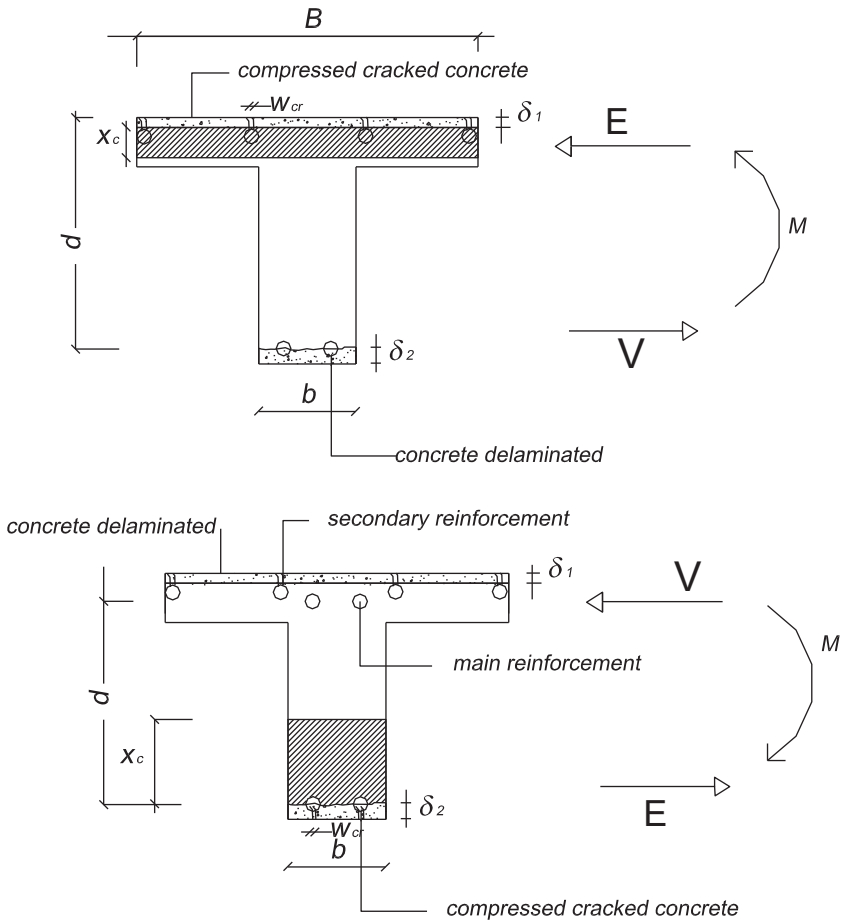

Fig. 3. Flexural section model for corroded R.C. beams.

The carbonation depth measured was in many cases between 33 and 45 mm, greater than the thickness of the concrete cover and the bars most frequently used, 12 or 14 mm in diameter, reduced to 9 and 11 after 30 years. In the case of the oldest constructions one of the two bars is straight up to the support and the other one is bent in the upper portion of the beam (typical reinforcement of a fixed beam). More recently, both bars are present in the support.

The present work examines the problem of corrosion and carbonation in R.C. floors for the past 50 years in the Mediterranean area which utilized R.C. beams cast in place having a T cross-section and interposed brick elements. An arch model is proposed to calculate the shear and flexural resistance of the corroded beam at a given time and to estimate the residual life of the structure for restoration purposes. No punching shear is considered. Also, the model does not take into account the presence of stirrups, because the only case examined is that of T beams forming a floor with low thickness.

2. Prediction of flexural and shear strength of R.C. T beams

R.C. cross-sections designed in practice are under-reinforced and the yield force in the tensile steel controls their flexural strength. By contrast, for over-reinforced cross-sections crushing of compressed concrete does not allow longitudinal bars to yield. For R.C. beams not damaged by corrosion processes it is possible to utilize the classical approach based on the plane section theory for flexure and an equivalent truss structure for shear strength prevision. By contrast, if damage due to corrosion process produces complete cover spalling with loss of bond, the plane section theory cannot be applied (see Fig. 3). In this case, the approach that can be applied is numerical [7], based on finite element analyses, or analytical. In this paper an analytical model is suggested based on arch mechanism resistance (Fig. 4), which links the crisis of the system to loss of anchorage in the support zone, to web crushing and to yielding of the main steel. In this model variation in beam geometry and in the properties of materials due to corrosive processes is considered.

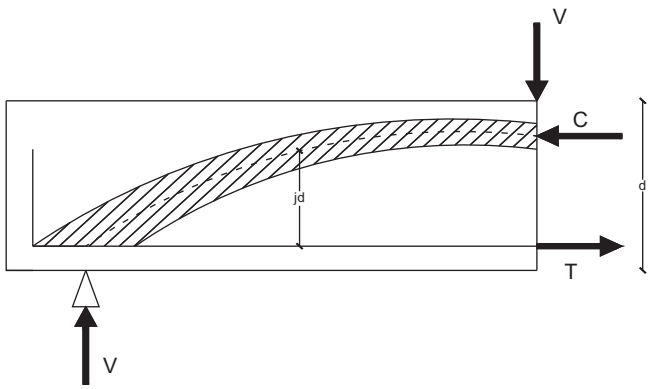

Fig. 4. Variation in dimensionless ultimate moment with geometrical ratio of longitudinal reinforcements ($a/d = L/4$; f_y 220 MPa, f_c = 15 MPa).

3. Flexural strength

For predicting flexural strength, the approach generally utilized in most codes (ACI 318 [8], Eurocode 2 [9], CAN CSA A23.3 [10]) is based on the plane section theory, which allows one to determine from the translation and rotation equilibrium of internal forces the position of the neutral axis and the ultimate moment.

In the elastic range and at rupture the neutral axis position (x_{cy}, x_{cu}) and the ultimate flexural strength M_u prove to be:

$$\frac{x_{cy}}{d} = \sqrt{(\rho \cdot n)^2 + 2 \cdot \rho \cdot n} - \rho \cdot n \tag{1}$$

with n the ratio between the elastic modulus of elasticity of steel and concrete E_s and E_c (modulus of elasticity of concrete assumed $E_c = 4700 \cdot \sqrt{f_c}$ as in [8]) and $\rho = A_s/(b \cdot d)$ the geometrical ratio of the main steel of area A_s in the cross-section with base b, effective depth d and cover δ.

$$\frac{x_{cu}}{d} = \frac{A_s \cdot f_y}{\alpha \cdot f_c \cdot \beta \cdot b \cdot d} \tag{2}$$

$$\frac{M_{us}}{b \cdot d^2 \cdot f_c} = \frac{A_s \cdot f_y}{b \cdot d \cdot f_c} \cdot \left(1 - \frac{1}{2} \cdot \beta \cdot \frac{x_{cu}}{d}\right) \tag{3}$$

α and β being the stress block coefficients assumed equal to 0.85 and 0.8, for normal strength concrete (lower values are suggested for high strength concrete because of their brittleness), f_y the yielding stress of the steel and f_c the compressive strength of the concrete.

4. Shear strength

For the concrete shear resistance contribution many international codes give clear indications (ACI 318 [8], Eurocode 2 [9], CAN CSA A23.3 [10]).

ACI 318 [8] suggests:

$$v_{uc} = \left(0.157 \cdot \sqrt{f'_c} + 17.2 \cdot \rho \cdot \frac{d}{a}\right) < 0.30 \cdot \sqrt{f'_c} \quad \text{in S.I. units} \tag{4}$$

with a the shear span of the beam.

The CSA [10] shear provisions were based on the shear resisting mechanism consisting of a free body diagram of the end portion of a beam. This portion intersects the flexural compression region and the longitudinal reinforcement and stirrups following the diagonal shear crack.

If the dowel action is neglected the shear strength equation is:

$$v_{uc} = \phi_c \cdot 0.4 \cdot \sqrt{f'_c} \leq 0.25 \cdot \phi_c \cdot f'_c \quad \text{in S.I. units} \tag{5}$$

where ϕ_c is the material reduction factors for concrete.

According to Eurocode 2 [9] the shear strength can be assumed as:

$$v_{uc} = 0.12 \cdot k \cdot (100 \cdot \rho \cdot f_c)^{1/3} \tag{6}$$

$$\text{with } k = 1 + \sqrt{\frac{200}{d}} \leq 2 \tag{7}$$

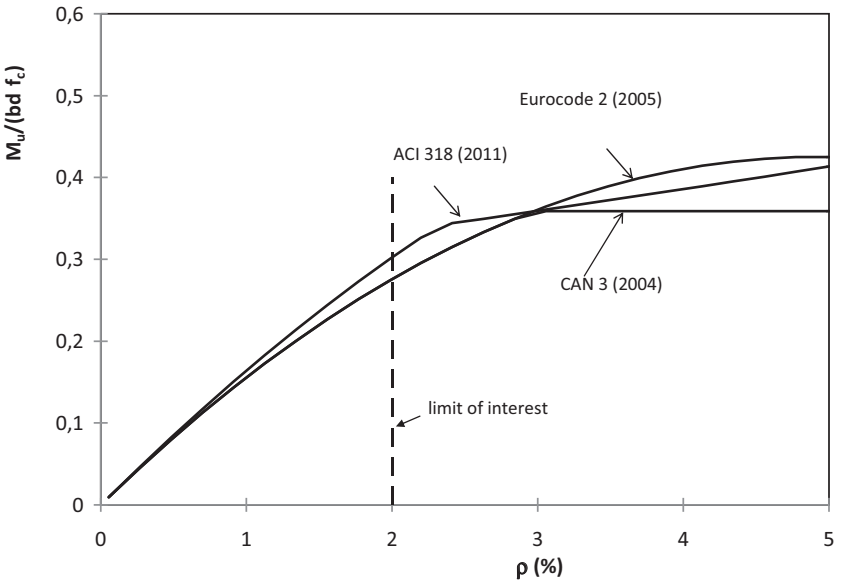

Fig. 5. Arch-resistant mechanism.

Applying the flexural and shear equations previously mentioned gives the graph in Fig. 5. The materials utilized had $f_c = 15$ MPa and $f_y = 220$ MPa; these are typical values for existing structures from the last two decades. This graph shows the variation in dimensionless ultimate moment with the geometrical ratio of the longitudinal reinforcement. The example shown refers to a T beam with height = $1/30L$ and $a/d = L/4$ (with $L = 4000$ mm) with a concentrated value load $V_{sd} = (q_{sd} \cdot L)/2$. This case corresponds in terms of maximum moment and shear force to a beam simply supported and subjected to a distributed load q_{sd}. In the same graph an upper limit of 2% for steel reinforcement is also given. It is evident that in most cases of interest of T beams with lightened slabs flexural failure is attained because $\rho < 2\%$.

5. Proposed model for corroded T members

The reference model for prediction of flexural and shear strength proposed here is the arch-resistant mechanism shown in Fig. 6. It reproduces the strength conditions of beams in which: the cover of bars in tension is completely spalled off; the cover of compressed bars is cracked and therefore the effective depth is $d - \delta$; the compressive strength is reduced by the biaxial state of stresses; the area of the main bars is reduced; the reduction in the yielding of the stress bars is negligible [4].

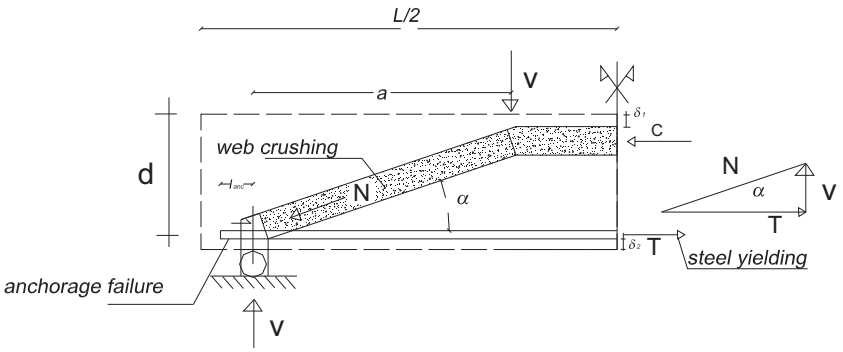

Fig. 6. Limit states for shear-to-moment interaction.

6. Effect of corrosion on strength degradation of materials

To verify whether there are ongoing corrosion processes, it has to be assumed that the thickness of the cover is equal to the carbonation depth S (mm), the latter being related to time t in years as suggested in [11]:

$$t = \left(\frac{\delta}{K}\right)^2 \tag{8}$$

Using Eq. (8) with K, a coefficient that depends on the ratio between water and cement and the strength of the concrete (in this case, for a normal strength concrete, K is assumed equal to 5), and $\delta = 20$ mm gives a time of 16 years.

After this time corrosion attack penetration can be measured experimentally with the gravimetric method or analytically as suggested in [12] in the form:

$$X = 0.0116 \cdot i_{corr} \cdot t \tag{9}$$

i_{corr} being the corrosion current density in the reinforcing bar expressed in $\mu A/cm^2$, ϕ the diameter and t the time in years.

Therefore the reduced diameter of the bar proves to be:

$$d_s(t) = \phi - 2 \cdot X \tag{10}$$

The maximum value of X is $\phi/2$.

In addition, the reduced area proves to be:

$$A_s(t) = n \cdot \frac{\pi \cdot [\phi - 2 \cdot X]^2}{4} \tag{11}$$

with n the number of bars at the support (the beam model was replaced with an arch-resistant model and therefore only the bars that were present in the tie were considered).

As suggested in [7], rust deposits produce lateral strain, which causes longitudinal micro-cracks and reduces the compressive strength. In the case of this kind of structure, because only a few bars with a small diameter are utilized, it appears reasonable to neglect this effect.

According to the model of Val [12] the depth of a pit, p(t), which is equivalent to the maximum penetration of pitting t years after the start of corrosion, can be evaluated as:

$$p(t) = 0.0116 \cdot i_{corr} \cdot t \cdot R \tag{12}$$

with $R = P_{max}/P_{av}$, where P_{max} is the maximum value of pit penetration and P_{av} the calculated value using Eq. (9).

Tuutti [5] suggests that R values are between 4 and 10 for 5 and 10 mm reinforcing bars of length 150–300 mm and in the next section a medium value of 5 will be assumed, according to Stewart [13]. The cross-sectional area of a pit, A_p, in a reinforcing bar, can be calculated according to the model of Fig. 7 of [12], as follows:

$$A_p(t) = \begin{cases} A_1 + A_2 & p(t) \le \dfrac{\phi}{\sqrt{2}} \\ \dfrac{\pi \cdot \phi^2}{4} - A_1 + A_2 & \dfrac{\phi}{\sqrt{2}} \le p(t) \le \phi \\ \dfrac{\pi \cdot \phi^2}{4} & p(t) \ge \phi \end{cases} \tag{13}$$

$$A_1 = \frac{1}{2} \cdot \left[2 \cdot \arcsin\left(\frac{2 \cdot p(t) \cdot \sqrt{1 - \left(\frac{p(t)}{\phi}\right)^2}}{\phi} \right) \cdot \left(\frac{\phi}{2}\right)^2 - 2 \cdot p(t) \cdot \sqrt{1 - \left(\frac{p(t)}{\phi}\right)^2} \cdot \left| \frac{\phi}{2} - \frac{p(t)^2}{\phi} \right| \right] \tag{14}$$

$$A_2 = \frac{1}{2} \cdot \left[2 \cdot \arcsin\left(\frac{2 \cdot p(t) \cdot \sqrt{1 - \left(\frac{p(t)}{\phi}\right)^2}}{2 \cdot p(t)} \right) \cdot p(t)^2 - 2 \cdot p(t) \cdot \sqrt{1 - \left(\frac{p(t)}{\phi}\right)^2} \cdot \frac{p(t)^2}{\phi} \right] \tag{15}$$

Therefore, the area of steel bars affected by pitting is:

$$A_s(t) = n \cdot \left(\frac{\pi \cdot \phi^2}{4} - A_p(t) \right) \ge 0 \tag{16}$$

Finally, in the presence of general corrosion and pitting the whole reduced area proves to be:

$$A_{sred}(t) = n \cdot \left\{ \frac{\pi \cdot [\phi - 2 \cdot X]^2}{4} - A_p(t) \right\} \tag{17}$$

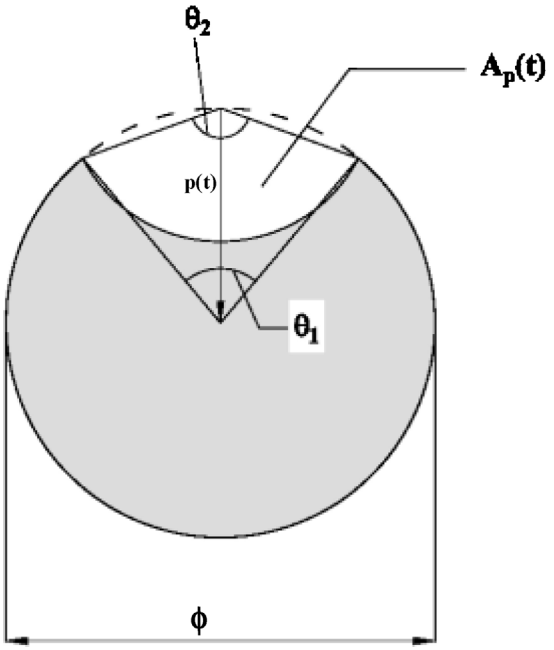

Fig. 7. Pitting model from Val [12].

Referring to bond strength it was verified that the post-peak bond strength was reduced with general corrosion and its variation can be expressed, as suggested in Bhargava et al. [14], in the form:

$$q_{res} = (0.77 - 0.037 \cdot X_p) \cdot \sqrt{f_c} \tag{18}$$

with X_p the corrosion level expressed as loss of mass in %. To calculate X_p it is necessary to define the mass M of the virgin and corroded bar. The mass of the virgin bar can be calculated as:

$$M_i = \frac{\pi \cdot \phi^2}{4}$$

The mass of the corroded bar is:

$$M_c = \frac{\pi \cdot d_s^2}{4} = \frac{\pi \cdot (\phi - 2 \cdot X)^2}{4}$$

Consequently, the loss of mass X_p can be calculated as:

$$X_p = \frac{\Delta M}{M_i} = \frac{M_i - M_c}{M_i} = 1 - \left(1 - \frac{(\phi - 2 \cdot X)^2}{\phi^2}\right) \tag{19}$$

And therefore substituting Eq. (19) into Eq. (18) gives:

$$q_{res} = \left\{0.77 - 0.037 \cdot \left[1 - \left(1 - \frac{2 \cdot X}{\phi}\right)^2\right]\right\} \cdot \sqrt{f_c} \tag{20}$$

7. Flexural and shear strength of corroded T beams

The simplified mechanism assumed for shear and flexural strength is the one shown in Fig. 6, in which the arch is substituted with a straight line. In this mechanism the following limit states are considered: crushing of web in compression; loss of anchorage in the support; yielding of longitudinal bars.

For a/the limit state governed by concrete crushing the ultimate axial force N in the concrete strut is:

$$N_c = \upsilon \cdot f_c \cdot b \cdot x_c \cdot \cos \alpha \tag{21}$$

where x_c is the position of the neutral axis derived from the translational equilibrium in the ultimate state and υ is the softening coefficient assumed as in the Swiss design code SIA [15] in the form:

$$\upsilon = 0.6 \cdot \left(\frac{30}{f_c}\right)^{0.33} \tag{22}$$

Table 1
Characteristics of analytical example (S.I. units).

B	H	s	ϕ	n_b	n	δ	L	a	f_c	f_y	l_{anc}
310	170	40	10	2	1	20	4000	1000	15	220	300

B, base of beam; H, height of beam; s, thickness of the flange; ϕ, bar diameter; n_{bars}, number of bars in one layer; n, number of bars in the support; δ, concrete cover thickness; L, maximum span; a shear span; f_c, mean value of concrete compressive strength; f_y, yield stress of longitudinal bar (or tie); l_{anc}, anchorage length.

and

$$\alpha = \arctan\left[\frac{j\cdot(d-\delta)}{a}\right] \tag{23}$$

j being the dimensionless internal arm assumed to be equal to 0.9.

The equilibrium of the forces at the support (see Fig. 6) gives:

$$V_c = N_c \cdot \sin\alpha \tag{24}$$

and therefore the ultimate shear stress related to the arch crushing is:

$$v_c = \frac{\upsilon\cdot f_c'}{2}\cdot\frac{x_{cu}}{d}\cdot\sin(2\alpha) \tag{25}$$

Imposing loss of bond due to corrosion in the anchorage zone from equilibrium of the internal forces at the support gives:

$$V_a = T_{ua}\cdot\tan\alpha = n\cdot\pi\cdot\phi_{red}\cdot l_{anc}\cdot q_{res}\cdot\tan(\alpha) \tag{26}$$

where ϕ_{red} is the equivalent reduced diameter.

l_{anc} being the anchorage length in the support.

The shear stress proves to be:

$$v_a = \frac{n\cdot\pi\cdot l_{anc}}{b\cdot d}\cdot\tan(\alpha)\cdot(\phi_{red}\cdot q_{res}) \tag{27}$$

If the limit state occurs due to yielding of the reduced area of steel bars we have:

$$V_s = T_{uy}\cdot\tan\alpha = A_{sred}\cdot f_y\cdot\tan(\alpha) \tag{28}$$

The shear stress is:

$$v_s = \frac{V_s}{b\cdot d} = \frac{A_{sred}\cdot f_y}{b\cdot d}\cdot\tan(\alpha) \tag{29}$$

Finally, the shear stress proves to be:

$$v_u = \min(v_c, v_a, v_s) \tag{30}$$

The ultimate bending moment is:

$$\frac{M_{us}}{b\cdot d^2\cdot f_c} = \frac{v_u}{f_c}\cdot\frac{a}{d} \tag{31}$$

To avoid brittle failure it is necessary that:

$$v_u \le \min(v_c, v_a) \tag{32}$$

It has to be stressed that if Eq. (28) is introduced in Eq. (31) we have:

$$\frac{M_{us}}{b\cdot d^2\cdot f_c} = \frac{A_{sred}\cdot f_y\cdot j}{b\cdot d\cdot f_c}\cdot\left(1-\frac{\delta}{d}\right) \tag{33}$$

To demonstrate the proposed model a numerical example is shown in Fig. 8. The data utilized are those given in Table 1. The corrosion current intensity was assumed to be 1 μA/cm^2 (according to Brite-Euram [16]), the pitting factor $R = 5$ (according to [13]), $K = 5$ (according to [11] for normal strength concrete) and CF = 1.35. For this application, the a/d ratio was set at $L/4$ with a concentrated load of $V_{sd} = (q_{sd}\cdot L)/2$. The cases shown in Fig. 8 refer to the use of two straight longitudinal bars prolonged up to the support with anchorage length 450 mm, and one straight longitudinal bar prolonged up to the support and one bent at $1/5L$.

In the graph the variations in ultimate moment (Eq. (32)) with time for a case of general and pitting corrosion are given. In the same graph, the design value derived by supposing a simply supported beam subjected to a dead load of 4.42 kN/m^2 and a service load of 2 kN/m^2 is also given. The safety factors for the dead and service load were 1.3 and 1.5 respectively as prescribed by Eurocode 2. The comparison shows that before 16 years no degradation occurs because of the thickness of the cover. During this time, the ultimate moment is due to the yielding of bars and its value is higher than the design value.

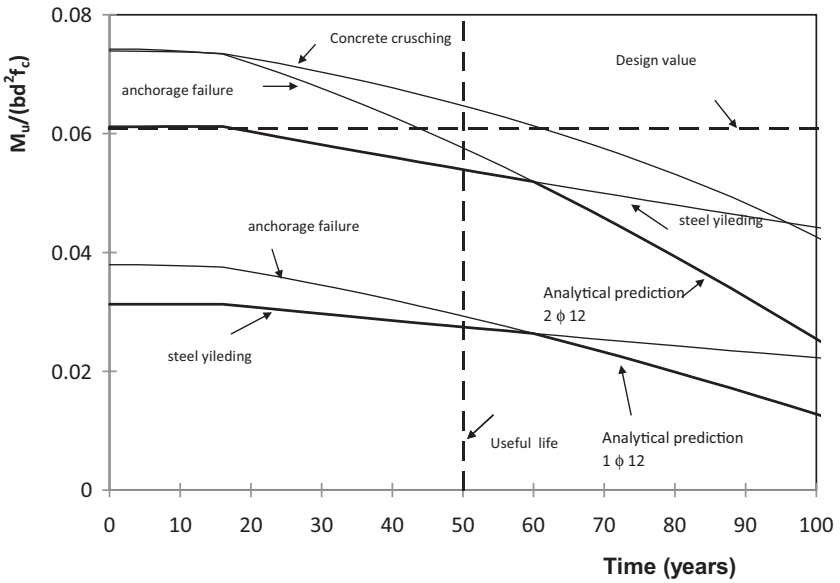

Fig. 8. Variation in dimensionless ultimate moment with time.

After 16 years anchorage failure governs the strength of the T beams because of the complete expulsion of the cover. At 50 years, 20% of the strength is lost with two bars and 10% with one bar, but in this case the strength value is lower than the design value because in the strength model the tie is only constituted by one bar and not by the two bars required with the flexural design based on the plane section theory. In both cases anchorage failure produces significant strength degradation and retrofitting is necessary. The choice of the calculus model strictly depends on the state of the floor: for severe damage the arch model is more suitable.

Retrofitting should do the following: integrate the loss of area of the longitudinal reinforcement up to the supports; ensure good anchorage in the support zone (e.g. by fixing new bars in the beam with epoxy resin); reconstruct the cover with a material having good bond with the old concrete and having similar mechanical characteristics to those of the old concrete.

8. Reference experimental research

In this section, the results of three experimental investigations carried out on R.C. beams with a T cross-section are utilized to validate the model [17–19].

Qin et al. [17] tested T beams strengthened in shear in flexure. All corroded and uncorroded beams were 2.7 m long and had a T cross-section with height 295 mm and flange with base 260 mm and thickness 100 mm. The web depth was 125 mm. The beams were reinforced at the bottom with 4 longitudinal bars with diameter 25 mm. Stirrups with diameter 8 mm, yielding stress 542 MPa and pitch 375 mm were utilized. The stirrups were corroded artificially with corrosion levels of 7% and 15% to represent medium and high corrosion levels respectively. The shear strengths were 145 kN, 152 kN and 155 kN respectively for beams with corrosion level 0, 7 and 15% and compressive cube strength of concrete of 26.8, 35.2 and 41.8 MPa, respectively.

Maaddawy and Chekfeh [18] tested T beams strengthened in shear and in flexure. All corroded and uncorroded beams were 3.00 m long and had a T cross-section with height 240 mm and flange with base 300 mm and thickness 50 mm. The web thickness was 120 mm depth. The beams were reinforced at the bottom with 4 longitudinal bars with diameter 16 and 25 mm. Stirrups with diameter 6 mm, yielding stress 344 MPa and no stirrups and stirrups with 120 mm pitch were utilised. The compressive cylindrical strength of the concrete was 32 MPa. The stirrups were corroded artificially with corrosion levels of 8% and 15%. The shear strength values measured experimentally were 109 and 113 kN for uncorroded beams, and 98 and 99 kN for corroded beams at 0.7% and 93 kN respectively with a corrosion level of 15%.

De Vecchi et al. [19] tested in flexure R.C. beams having a T cross-section and the geometry is shown in Fig. 9. Three different types of T beams were examined. Each type consisted of three identical specimens. The first type was reinforced in the bottom part of the web with smooth bars having 10 mm diameter, in the presence of bricks. The other two were reinforced with smooth bars having 8 mm diameter, in the absence of bricks. One series had no cover, while the other series had a cover reconstructed with thixotropic mortar. The aim of this study was to simulate the conditions of reduction of steel area occurring during corrosion process consisting in reduction of the area of the bars, concrete cover spalling and breaking of brick blocks. Concrete had compressive strength $f_c = 20$ MPa, and steel bars had yield stress $f_y = 450$ MPa. The loading scheme shown in Fig. 10 is a three-point bending test with a span between supports of 1875 mm and $a/d = 4.68$.

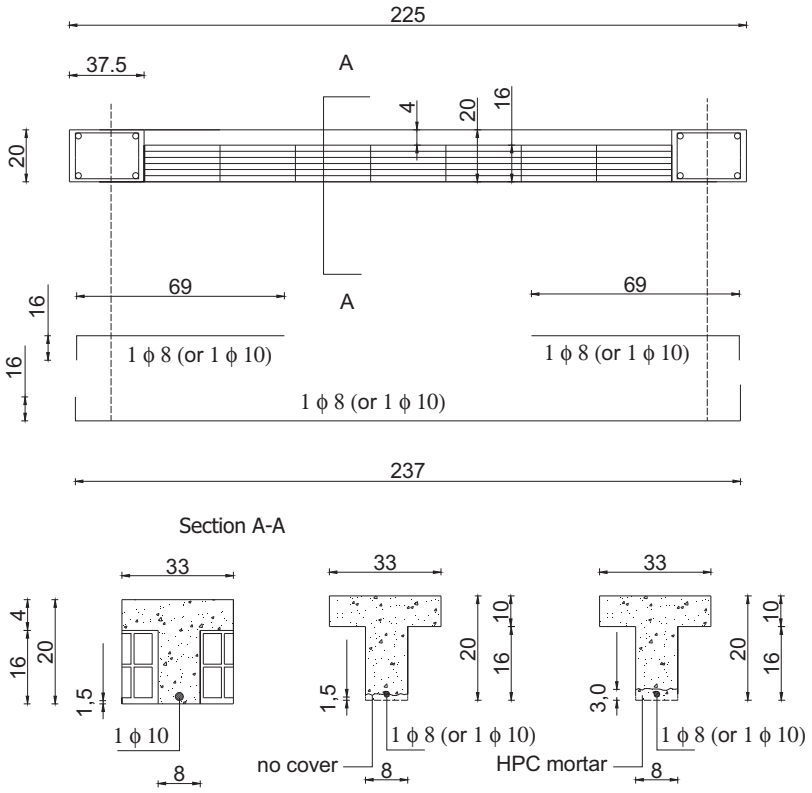

Fig. 9. Prototype tested.

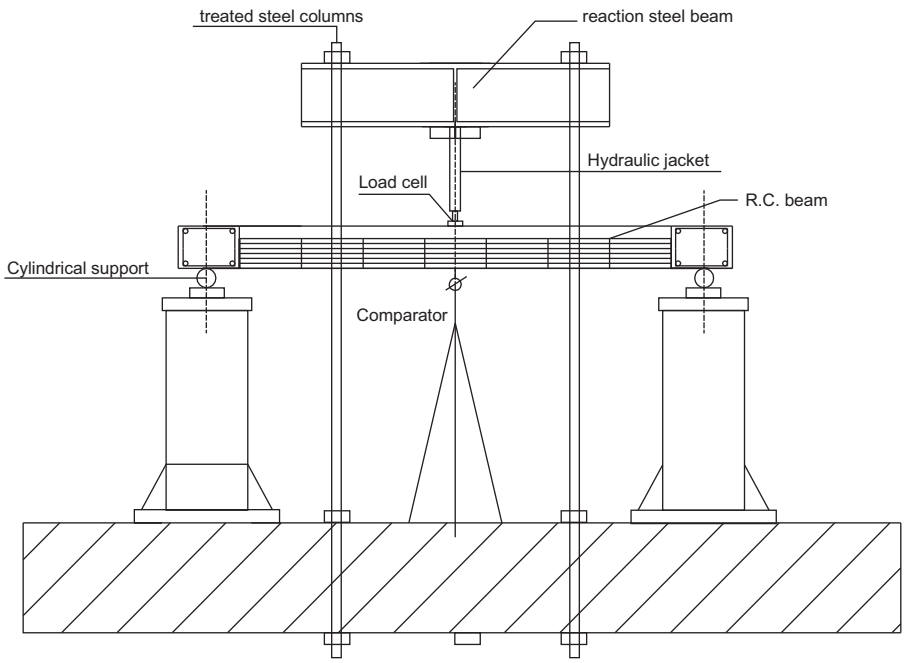

Fig. 10. Test setup.

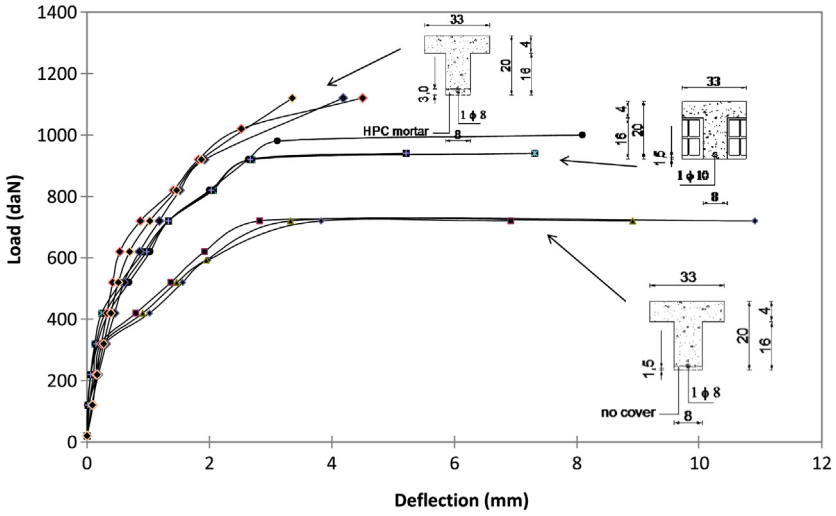

Fig. 11. Load-deflection curves of T beams.

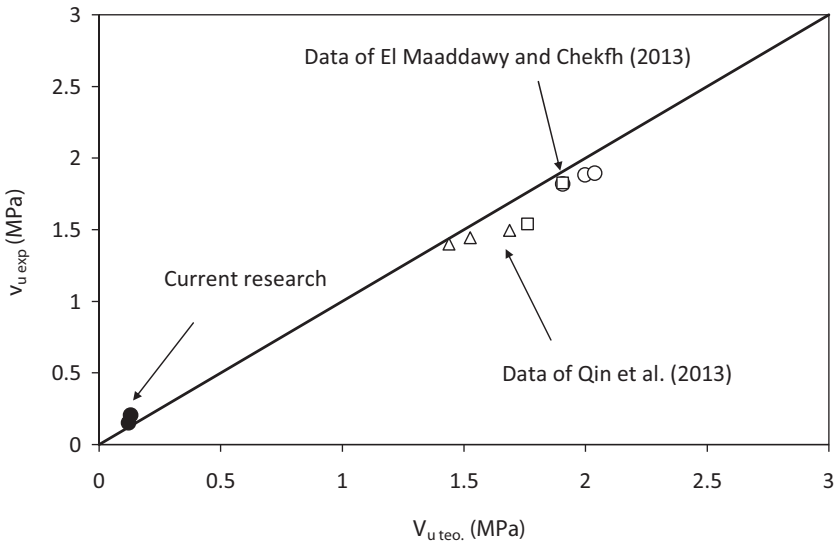

Fig. 12. Strength and area reduction with increase in time.

The specimens were supported by steel cylinders and loaded by means of a hydraulic jack with a load cell. The deflections were recorded though a comparator placed in the middle lower portion of the beam as shown in Fig. 10.

Fig. 11 shows the load–deflection curves for the different specimens investigated. The test results show that the specimens with small diameter bars had less strength than the ones having higher diameter bars and lower initial stiffness. The crisis was due to yielding of the main steel; no slippage was observed at the support, even for specimens without concrete cover. With reconstruction of the concrete cover with high performance mortar an increase in the initial stiffness and in the flexural strength was observed; by contrast, the failure mode was brittle because the contribution in traction due to the mortar was higher than the yield force of the small diameter bars. This is an important aspect to be reckoned with and to be avoided in order to use high-strength materials for reinforcement.

Fig. 12 shows the variation in experimental shear and flexural strength versus the analytical prediction for all cases examined. Comparison of the theoretical and experimental results shows good agreement both in terms of strength variation and failure mode.

9. Conclusions

In the present paper, a simplified analytical model based on arch-resistant mechanism to derive the flexural and the shear strength of corroded T beams cast in place of lightened R.C. slabs forming floors is presented and discussed.

Preliminary research on the effects of corrosion on the properties of materials highlights that the main effects due to general corrosion and pitting are: reduction in steel area and ductility; loss of bond strength; concrete compressive strength degradation.

The expressions derived for shear strength considered several possible limit states (anchorage failure, concrete crushing of compressed strut) and reduction in the geometrical and mechanical parameters (cross-section area of section, area of steel bar bond and compressive strength).

All the expressions derived allow hand calculation and have a clear physical meaning. Finally, comparison with existing experimental data was satisfactory in terms of both strength prevision and failure modes.

Acknowledgements

This work has benefited from material deriving from the 2010-2013 Research Project ReLUIS (Rete dei Laboratori di Ingegneria Sismica), AT 1, Task 1.1.2: Strutture in Cemento Armato ordinarie e prefabbricate.

References

[1] L. Santarella, Handbook of Reinforced Concrete, Edizioni Hoepli, Italy, 1932 (only available in Italian).
[2] S. Ting, A. Nowak, Effect of reinforcing steel area loss on flexural behavior of RC beams, ACI J. Struct Eng. 88 (3) (1991) 309–314.
[3] J. Rodriguez, L.M. Ortega, J. Casal, Load carrying capacity of concrete structures with corroded reinforcement, Constr. Build. Mater. 11 (4) (1997) 239–248.
[4] A.A. Almusallam, Effect of degree of corrosion on the properties of reinforcing steel bars, Constr. Build. Mater. 15 (2001) 361–368.
[5] K. Tuutti, Corrosion of Steel in Concrete. Fo 4.82, Swedish Cement and Concrete Research Institute, Stockholm, Sweden, 1982.
[6] H.W. Song, B. Saraswathy, Corrosion monitoring of reinforced concrete structures – a review, Int. J. Electrochem. Sci. 2 (2007) 1–28.
[7] D. Coronelli, P. Gambarova, Structural assessment of corroded reinforced concrete beams: modeling guidelines, ASCE J. Struct. Eng. (2004, August) 1214–1224.
[8] ACI Committee 318, Building Code Requirements for Structural Concrete and Commentary, American Concrete Institute, Framington Hills, MI, 2011.
[9] Eurocode 2: Design of Concrete Structures – Part 1: General Rules and Rules for Buildings, European Committee for Standardization (CEN), 2005.
[10] Canadian Standards Association, CAN CSA A23.3-04 Design of concrete structures, CSA, Rexdale, Ontario, 2004.
[11] P. Pedeferri, L. Bertolini, La durabilità del calcestruzzo armato, McGraw-Hill, 2000 (only available in ITALIAN).
[12] D.V. Val, Deterioration of strength of RC beams due to corrosion and its influence on beam reliability, ASCE J. Struct. Eng. 133 (9) (2007) 197–1306.
[13] M.G. Stewart, Mechanical behaviour of pitting corrosion of flexural and shear reinforcement and its effect on structural reliability of corroding RC beams, Struct. Saf. 31 (2009) 19–30.
[14] K. Bhargava, A. Ghosh, Y. Mori, S. Ramanujam, Suggested empirical models for corrosion-induced bond degradation in reinforced concrete, J. Struct. Eng. 134 (2) (2008) 221–230.
[15] SIA 262. Concrete Structures, Code, Swiss society of Engineers and Architects, Zurich, 2003, pp. 90.
[16] Brite-Euram project: Service life of concrete structures BE-4062, 1992.
[17] S. Qin, S. Dirar, J. Yang, A. Chan, M. Elshafie, CFRP shear strengthening of reinforced-concrete T-beams with corroded shear links, J. Compos. Constr. (2013), 10.1061/(ASCE)CC.1943-5614.0000548, 04014081.
[18] El Maaddawy, M.Y. Chekfh, Effectiveness of NSM-GFRP strengthening to upgrade shear capacity of T-beams with corroded stirrups, ACI Struct. J. 110 (September–October (5)) (2013).
[19] A. De Vecchi, G. Zingone, G. Campione, R. Corrao, S. Colajanni, A. Giammanco, Joists and floors, Modulo 307 (2005) 1206–1209 (only available in Italian).